Journal of the American College of Cardiology Vol. 55, No. 18, 2010

ISSN 0735-1097/$36.00
doi:10.1016/j.jacc.2010.01.028

Multicenter Trial of High-Speed Versus Conventional Single-Photon Emission Computed Tomography Imaging

Quantitative Results of Myocardial Perfusion and Left Ventricular Function

Tali Sharir, MD,* Piotr J. Slomka, PHD,† Sean W. Hayes, MD,† Marcelo F. DiCarli, MD,‡ Jack A. Ziffer, MD,§ William H. Martin, MD,‖ Dalia Dickman, PHD,¶ Simona Ben-Haim, MD,# Daniel S. Berman, MD†

Tel Aviv, Israel; Los Angeles, California; Boston, Massachusetts; Miami, Florida; Nashville, Tennessee; Caesarea, Israel; and London, United Kingdom

Objectives This prospective, multicenter trial compared quantitative results of myocardial perfusion imaging and function using a high-speed single-photon emission computed tomography (SPECT) system with those obtained with conventional SPECT.

Background A novel SPECT camera was shown in a pilot study to detect a similar amount of myocardial perfusion abnormality compared with conventional SPECT in one-seventh of the acquisition time.

Methods A total of 238 patients underwent myocardial perfusion imaging with conventional and high-speed SPECT at 4 U.S. centers. An additional 63 patients with a low pre-test likelihood of coronary artery disease underwent myocardial perfusion imaging with both technologies to develop method- and sex-specific normal limits. Rest/stress acquisition times were, respectively, 20/15 min and 4/2 min for conventional and high-speed SPECT. Stress and rest quantitative total perfusion deficit, post-stress left ventricular end-diastolic volume, and ejection fraction were derived for the 238 patients by the 2 methods.

Results High-speed stress and rest total perfusion deficit correlated linearly with conventional SPECT total perfusion deficit ($r = 0.95$ and 0.97, respectively, $p < 0.0001$), with good concordance in the 3 vascular territories (kappa statistics for the left anterior descending coronary artery, left circumflex coronary artery, and right coronary artery were 0.73, 0.73, and 0.70, respectively; >90% agreement). The percentage of ischemic myocardium by both imaging modalities was significantly larger in patients with a high coronary artery disease likelihood than in those with a low and intermediate likelihood ($p < 0.001$). The average amount of ischemia was slightly but significantly larger by high-speed SPECT compared with conventional SPECT in high-likelihood patients ($4.6 \pm 4.6\%$ vs. $3.9 \pm 4.0\%$, respectively; $p < 0.05$). Post-stress ejection fraction and end-diastolic volume by the 2 methods were linearly correlated ($r = 0.89$ and 0.97, respectively).

Conclusions The high-speed SPECT technology provides quantitative measures of myocardial perfusion and function comparable to those with conventional SPECT in one-seventh of the acquisition time. (J Am Coll Cardiol 2010;55:1965–74) © 2010 by the American College of Cardiology Foundation

Single-photon emission computed tomography (SPECT) myocardial perfusion imaging (MPI) plays a central role in the diagnosis and prognostic evaluation of coronary artery disease (CAD) and in guiding patient management. Its basic technology has not changed in more than 50 years (1).

A new, compact gamma camera system using a novel design of photon acquisition and image reconstruction was recently developed (Spectrum Dynamics, Ceasaria, Israel) (2–5). This technology uses 9 pixilated solid-state cadmium

See page 1975

From the *Assuta Medical Center, Tel Aviv, Israel; †Cedars Sinai Medical Center, Los Angeles, California; ‡Brigham and Women's Hospital, Boston, Massachusetts; §Baptist Hospital of Miami, Miami, Florida; ‖Vanderbilt University Medical Center, Nashville, Tennessee; ¶Spectrum Dynamics, Caesarea, Israel; and the #UCL Institute of Nuclear Medicine, London, United Kingdom. Dr. Sharir is an investigator and consultant for Spectrum Dynamics. Dr. Slomka receives royalties from the software used in the study. Dr. DiCarli has received research grants from GE, Siemens, Bracco, and Astellas. Dr. Ziffer has equity in and has received honoraria from Spectrum Dynamics, and is a consultant with Lantheus, Astellas, and RCARIA. Dr. Martin is a consultant to Spectrum Dynamics. Dr. Dickman is an employee of Spectrum Dynamics. Dr. Ben-Haim is an investigator and consultant for Spectrum Diagnostics. Dr. Berman is a shareholder in Spectrum Dynamics and receives royalties from the software employed in the study.

Manuscript received July 27, 2009; revised manuscript received January 4, 2010, accepted January 11, 2010.

JACC Vol. 55, No. 18, 2010
May 4, 2010:1965–74

Abbreviations and Acronyms

BHM = Baptist Hospital of Miami
BMI = body mass index
BWH = Brigham and Women's Hospital
CAD = coronary artery disease
CSMC = Cedars-Sinai Medical Center
EDV = end-diastolic volume
EF = ejection fraction
LVEF = left ventricular ejection fraction
MPI = myocardial perfusion imaging
SPECT = single-photon emission computed tomography
TPD = total perfusion deficit

zinc telluride crystal detector columns, wide-angle tungsten collimators, and region of interest–centric scanning. A recent pilot study (6) demonstrated a highly linear correlation between the magnitude of stress and rest perfusion abnormality using high-speed SPECT and a conventional system.

We conducted a prospective, multicenter clinical trial to compare the ability of high-speed SPECT with that of conventional SPECT in detecting myocardial perfusion abnormalities in patients referred for evaluation of CAD in multiple laboratories using quantitative analysis of myocardial perfusion and function.

Methods

Study design. We hypothesized that the extent and severity of perfusion abnormalities detected by high-speed SPECT would be similar to those detected by conventional SPECT in patients with an intermediate to high likelihood of CAD. We further hypothesized that among subjects with a low likelihood of CAD, perfusion defects would be similar with both technologies.

We also postulated that similar findings would be found when comparing the 2 modalities in each of the medical centers participating in the trial.

Study population. The study was conducted at 4 institutions: Cedars-Sinai Medical Center (CSMC), Los Angeles, California; Brigham and Women's Hospital (BWH), Boston, Massachusetts; Baptist Hospital of Miami (BHM), Miami, Florida; and Vanderbilt University Medical Center, Nashville, Tennessee. Based on availability of the equipment and technical staff, a total of 301 consecutive consenting patients undergoing clinically ordered myocardial perfusion SPECT were recruited. The data for 63 patients (32 women, 31 men) with visually normal scans and a low (<15%) likelihood of disease were used for the development of separate normal limits for high-speed SPECT and conventional SPECT. Of the 63 patients, 25 (39.7%) were asymptomatic and 38 (60.3%) had history of atypical chest pain. Eighteen (28.6%) patients had a history of hypertension, 20 (31.7%) had hypercholesterolemia, and 5 (7.9%) were current smokers. None of the patients had a history of diabetes mellitus. These patients underwent rest/stress (exercise, n = 53; adenosine, n = 10) Tc-99m sestamibi (n = 45) or Tc-99m tetrofosmin (n = 18) SPECT by both technologies. An additional 238 patients were recruited for validation of high-speed SPECT, of whom 43 had a low likelihood of CAD (<15%), 84 had an intermediate likelihood (15% to 85%), and 111 had a high (>85%) likelihood. Quantitative measurements of myocardial perfusion by high-speed SPECT based on the newly developed normal limits were assessed in these 238 patients (105 women, 133 men) and compared with quantitative measurements with conventional SPECT.

Exclusion criteria were nonischemic cardiomyopathy, significant valvular heart disease, left bundle branch block, paced ventricular rhythm, and uncontrolled congestive heart failure.

A total of 9% (30 of 331) of patients were excluded from the study due to technical reasons. Of these, 7.9% (26 of 331) were high-speed SPECT related and 2.1% were conventional SPECT related. The study was approved by the institutional review board at each center, and all patients gave written informed consent.

Pre-test likelihood of CAD. The pre-test CAD likelihood was calculated using CADENZA software, based on sequential Bayesian analysis of age, sex, symptom classification, CAD risk factors, and treadmill stress test results (7). For patients with previous myocardial infarction or revascularization, the pre-test likelihood was set at 100%. For patients who underwent pharmacologic stress testing, the pre-test likelihood was calculated without using the stress test parameters.

Stress protocols and radiopharmaceuticals. Table 1 summarizes the stress protocols and radiopharmaceuticals used at the 4 medical centers. Patients underwent treadmill exercise testing (n = 146) or a pharmacologic stress testing using adenosine (n = 82) or dobutamine (n = 7). Patients

Table 1 Stress Protocols and Radiopharmaceuticals

	CSMC	BWH	BHM	VUMC	All	p Value
n	61	59	63	55	238	—
Treadmill exercise	37 (61%)	42 (71%)	34 (54%)	33 (60%)	146 (61%)	NS
Adenosine stress	24 (39%)	16 (27%)	24 (38%)	18 (33%)	82 (34%)	NS
Dobutamine stress	—	—	5 (5%)	3 (5%)	7 (3%)	NS
Tc-99m sestamibi	44 (72%)	59 (100%)	62 (98%)	—	166 (70%)	<0.001
Tc-99m tetrofosmin	—	—	—	55 (100%)	55 (23%)	—
Dual isotope	18 (30%)	—	—	—	18 (8%)	—

BHM = Baptist Hospital of Miami; BWH = Brigham and Women's Hospital; CSMC = Cedars-Sinai Medical Center; VUMC = Vanderbilt University Medical Center.

were injected with 370 MBq (10 mCi) Tc-99m sestamibi or tetrofosmin at rest, and conventional SPECT imaging was initiated 1 h later, followed by high-speed SPECT imaging. Then 1,110 MBq (30 mCi) Tc-99m sestamibi or tetrofosmin was injected at peak stress, and conventional SPECT imaging was started 15 to 30 min later, followed by high-speed SPECT imaging. Nineteen patients underwent a dual-isotope protocol: rest thallium-201 (74 MBq)/stress Tc-99m sestamibi (1,110 MBq). The resting thallium-201 data for these patients were excluded from the analysis.

Acquisition protocol of conventional SPECT. Conventional SPECT images were acquired in the supine position using a 2-detector 90° camera: E-CAM (Siemens, Hoopeston, Illinois) at CSMC and BWH; Precedence (Philips, Bothell, Washington) at MBH; Ventri (GE, Milwaukee, Wisconsin) at Vanderbilt University Medical Center, using 60 or 64 projections over a 180° orbit and low-energy, high-resolution collimation. Electrocardiographic gating was performed using 16 frames/cycle at CSMC and 8 frames/cycle at the other centers. Total imaging time was ~20 min and ~15 min for resting and stress acquisitions, respectively.

Summed projections were reconstructed with an iterative maximum likelihood expectation maximization algorithm (8–10), 12 iterations, and a Butterworth analytic filter (5.0 order, 0.66 and 0.55 cutoff frequency for stress and rest images, respectively). Gated projections were reconstructed using filtered back-projection and a Butterworth pre-filter (5.0 order, 0.44 cutoff frequency).

High-speed SPECT technology and acquisition protocol. A description of the high-speed SPECT technology (D-SPECT, Spectrum Dynamics, Caesarea, Israel) was recently published (5). Briefly, the system uses 9 pixilated cadmium zinc telluride crystal detector columns mounted vertically spanning a 90° geometry. Each of the columns consists of 1,024 (16 × 64) 5-mm thick cadmium zinc telluride crystal elements (2.46 × 2.46 mm). Square-hole tungsten collimators are fitted to each of the detectors, which are shorter than conventional low-energy, high-resolution collimators, yielding significantly better geometric speed. Data are acquired by the detectors rotating in synchrony, focusing on the heart and saved in list mode. The resultant loss in spatial resolution related to the collimators used is compensated for by acquiring data from multiple projections (>1,000) and using a proprietary Broadview reconstruction algorithm based on the maximum likelihood expectation maximization algorithm (8–10).

Images were acquired with the patient in a semirecumbent position. A 10-s pre-scan acquisition was performed to identify the location of the heart and to set the angle limits of scanning for each detector (region of interest–centric scanning). A 4-min rest acquisition (120 projections per detector, 2 s per projection) was performed after resting conventional SPECT imaging, and a 2-min acquisition (1 s per projection) followed the conventional post-stress SPECT imaging. Summed and gated projections were reconstructed with an iterative maximum likelihood expectation maximization algorithm using 7 and 4 iterations, respectively.

Exercise and pharmacologic stress protocols. Patients were asked to discontinue beta-blockers and calcium antagonists 48 h and nitrates 24 h before testing. A symptom-limited treadmill exercise test was performed, using the Bruce protocol. Tc-99m sestamibi or tetrofosmin was injected at peak stress, and exercise continued at the same level for 1 min and for 2 min at 1 level lower. Before adenosine stress, patients were instructed to avoid caffeine-containing products for 24 h before the test. Adenosine (140 μg/kg/min) was infused over 4 to 5 min, and the radioisotope was injected at the end of the second or third minute. Whenever possible, patients performed low-level treadmill exercise during adenosine infusion.

Seven of the 238 patients underwent dobutamine stress, starting with 10 μg/kg/min and up-titrated every 3 min by 10 μg/kg/min up to 40 μg/kg/min.

Quantitative data processing. Image data were processed at the CSMC nuclear core laboratory by a senior technologist under the supervision of the core laboratory codirector (S.H.). High-speed and conventional SPECT images were processed separately, with blinding to the corresponding modality and clinical information. Manual adjustments of myocardial contours were performed in cases with misplaced myocardial contours or valve plane (~10% of the cases for high-speed and conventional SPECT).

Quantitative analysis of myocardial perfusion. Normal limits for stress and rest myocardial perfusion were generated separately for high-speed and conventional SPECT, using images from the same patients (normal group). These normal limits were developed using a simplified method, without the need for visual scoring of abnormal scans, as previously described (11). Briefly, contours of the left ventricle were generated using an ellipsoidal model, and polar-map samples were extracted (12). Count normalization, using an iterative search for minimal absolute count difference in the normal region, was applied (13), and average deviations were calculated. A threshold of 3.0 average deviations (equivalent to approximately 2.5 SDs) was applied to define hypoperfusion (11).

High-speed and conventional SPECT images of the validation group were quantitatively analyzed using the method-specific normal limits developed in the 63 patients with a low CAD likelihood. The total perfusion deficit (TPD) of the stress and resting images was generated, representing the defect extent and severity and expressed as a percentage of the left ventricular myocardium (13). The theoretical maximum value for TPD is 100% for a case with no uptake (<70% below normal) in the entire left ventricular myocardium.

Quantitative analysis of gated SPECT. Post-stress left ventricular ejection fraction (LVEF) was automatically obtained using QGS software (CSMC) for conventional gated SPECT images (12), whereas high-speed SPECT gated

JACC Vol. 55, No. 18, 2010
May 4, 2010:1965–74

Table 2 Clinical Characteristics

Characteristics	Medical Center					
	CSMC (n = 61)	BWH (n = 59)	MBH (n = 63)	VUMC (n = 55)	All (n = 238)	p Value
Male	43 (70)	28 (47)	34 (54)	28 (51)	133 (56)	0.045
Age, yrs	60 ± 12	63 ± 10	56 ± 13	58 ± 13	60 ± 12	0.008
BMI	27 ± 5	29 ± 6	33 ± 10	31 ± 9	30 ± 8	<0.001
Hypertension	40 (67)	42 (71)	46 (73)	36 (65)	165 (69)	0.76
Diabetes mellitus	15 (25)	14 (24)	19 (30)	13 (24)	61 (26)	0.8
Hypercholesterolemia	41 (67)	41 (69)	27 (43)	31 (56)	140 (59)	0.009
History of CAD	26 (43)	30 (51)	21 (33)	20 (36)	97 (41)	0.21
History of MI	16 (26)	20 (34)	16 (25)	11 (20)	63 (26)	0.41
History of PCI	18 (30)	23 (39)	14 (22)	10 (18)	65 (27)	0.06
History of CABG	4 (7)	7 (12)	5 (8)	9 (16)	25 (11)	0.3
Typical angina or SOB	2 (34)	18 (31)	12 (19)	24 (44)	75 (32)	0.024
Pre-test CAD likelihood	0.58 ± 0.43	0.71 ± 0.36	0.50 ± 0.41	0.66 ± 0.34	0.60 ± 0.39	0.016

Values are n (%) or mean ± SD.

BMI = body mass index; CABG = coronary artery bypass grafting; CAD = coronary artery disease; MI = myocardial infarction; PCI = percutaneous coronary intervention; SOB = shortness of breath; other abbreviations as in Table 1.

images were quantitatively analyzed using a modified version of QGS accounting for higher resolution and better visibility of the myocardial base.

Statistical analysis. Continuous variables are presented as mean ± SD. Comparisons among centers were performed using the chi-square test for categorical variables and 1-way analysis of variance for continuous variables. A p value <0.05 was considered significant. Correlations between TPD by high-speed versus conventional SPECT were evaluated by linear regression, and differences between the 2 methods were assessed by Bland-Altman analysis (14). Concordance between the methods was assessed using kappa analysis.

Perfusion abnormality as a function of the pre-test likelihood was compared using a paired *t* test, with $p < 0.05$ considered significant. Where distributions were non-normal, Wilcoxon signed rank tests were used, and correlations were confirmed using the Spearman rank method.

Results

Patient characteristics. The clinical characteristics of the 238 patients in the validation group are summarized in Table 2. Fifty-six percent of patients were males; the average age was 60 ±12 years, and the average body mass index (BMI) was 30 ± 8 kg/m^2. Significant differences among the 4 medical centers were observed in the proportion of males, age, BMI, frequency of hypercholesterolemia, and incidence of typical angina or shortness of breath. The proportion of males ranged from 47% at BWH to 70% at CSMC ($p = 0.045$). The overall age range was 22 to 87 years, and the mean age ranged from 56 ± 13 years at BHM to 63 ± 10 years at BWH ($p = 0.008$). The mean BMI was lowest at CSMC (27 ± 5 kg/m^2) and highest at BHM (33 ± 10 kg/m^2) ($p < 0.001$). The overall pre-test likelihood of CAD was significantly different among the centers, ranging from 0.50 ± 0.41 at BHM to 0.71 ± 0.36 at BWH ($p = 0.016$).

Normal limits of myocardial perfusion. Mean and SD values of normalized stress perfusion for high-speed and conventional SPECT imaging in 17 segments of the left ventricle in the 31 men and 32 women with a low CAD likelihood are shown in Figure 1. With the high-speed system in men, higher count rates were observed in the anterior and mid-inferior inferoseptal segments, whereas in women, higher count rates were seen in the anterior wall but lower counts in the inferior segments. Similar differences were observed in the resting normal limits of men and women.

Perfusion abnormality: correlation with conventional-SPECT. Categorizing patients into 3 groups of stress TPD (normal, <5%; mild-moderate, 5% to 15%, and severe abnormality, >15%) (Table 3) demonstrated that by conventional SPECT, 162 patients had normal MPI and 76 had abnormal MPI (46 mild or moderate and 30 severe defects). By high-speed SPECT, 169 patients had normal MPI and 69 abnormal MPI (39 mild or moderate and 30 severe perfusion deficits). Good concordance between the methods with 83.6% agreement and kappa = 0.65 ($p < 0.001$) was observed.

Quantitative TPD by high-speed SPECT demonstrated linear correlation with conventional SPECT for stress (Fig. 2A) and rest (Fig. 2B) images, over a wide range of MPI abnormality (Pearson r = 0.95 and 0.97, respectively; $p < 0.0001$; Spearman correlation coefficients 0.67 and 0.64 for stress and rest, respectively; $p < 0.001$).

Bland-Altman analysis demonstrated small mean TPD differences between conventional and high-speed SPECT and a relatively small SD for the stress (Fig. 3A) and rest (Fig. 3B) images (−0.0007 ± 3.2 and 0.4 ± 2.1, respectively), with no correlation between the differences and mean TPD.

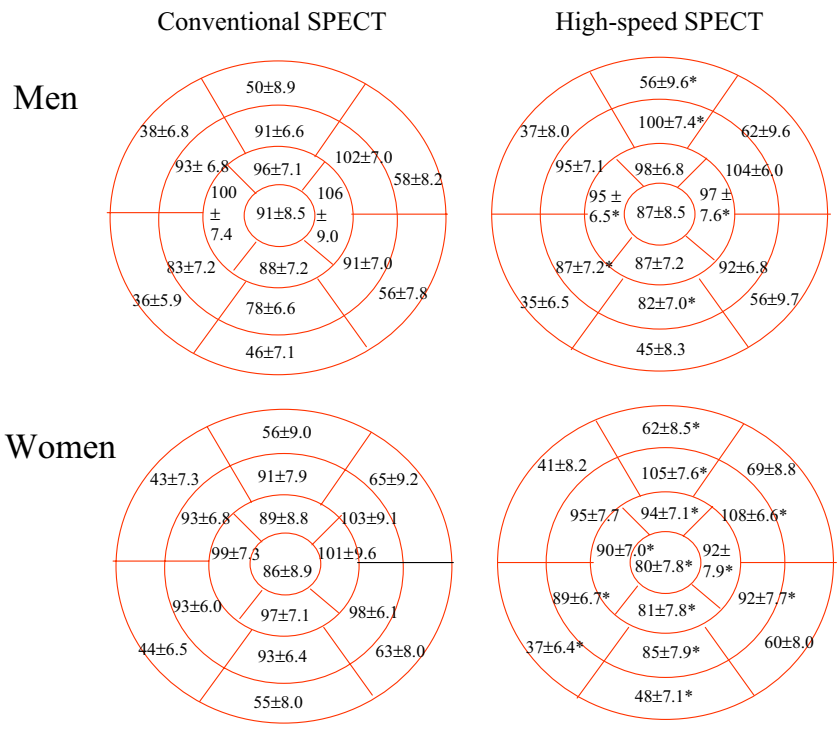

Figure 1 Segmental Variability of Relative Myocardial Perfusion by High-Speed SPECT Versus Conventional SPECT

Men **(top)** and women **(bottom)**. Mean ± SD values in 17 myocardial segments are shown.
*p < 0.05 versus corresponding segment in conventional single-photon emission computed tomography (SPECT).

The Wilcoxon signed rank test was insignificant for stress TPD by high-speed versus conventional SPECT (p = 0.25), but significant for rest TPD comparison (p = 0.02).

Center-based analysis demonstrated linear correlation between high-speed TPD and conventional TPD in the stress and rest images in all participating centers (Table 4).

Analysis by coronary artery territories revealed good concordance in all 3 territories (Table 5).

Magnitude of perfusion abnormality as a function of pre-test likelihood of CAD. The magnitude of stress TPD by both high-speed and conventional SPECT images was significantly greater in patients with a high pre-test likelihood of CAD than a low or intermediate likelihood (p < 0.001) (Fig. 4A). No difference between the methods was observed within each of the likelihood categories. The average amount of ischemia (calculated as the difference between stress and rest TPD) among patients with a high likelihood was significantly higher for high-speed SPECT compared with conventional SPECT (4.6 ± 4.6 vs. 3.9 ± 4.0, respectively; p < 0.05) and similar among patients with low and intermediate likelihood (Fig. 4B).

Defining the stress-rest TPD difference of ≥5% as a reversible defect and rest TPD ≥7% as a fixed defect demonstrated 81.5% agreement between the 2 methods among patients with intermediate and high CAD likelihood (Table 6). Of the 32 patients with reversible or partially reversible defects by conventional SPECT, 4 had fixed defects and 8 were normal by high-speed SPECT. Conversely, of the 41 patients with reversible or partially reversible defects by the high-speed technology, 10 had fixed defects and 11 were normal by conventional SPECT (p = 0.37).

Correlation of post-stress end-diastolic volume (EDV) and ejection fraction (EF). Gated data of high-speed and conventional SPECT were obtained in 220 of the 238 patients. Figure 5 demonstrates linear correlation between EDV by high-speed and conventional SPECT (r = 0.96). The average post-stress LVEF for the entire group was slightly but significantly higher for high-speed compared with conventional SPECT (63.2 ± 13.15 vs. 62.2 ± 12.6, p = 0.017). The correlation between LVEF by the 2

Table 3 Concordance of Stress Perfusion Findings

	High-Speed SPECT			
Conventional SPECT	Normal	Mild-Moderate Perfusion Defect	Severe Perfusion Defect	Total
Normal	149	13	0	162
Mild-moderate perfusion defect	20	23	3	46
Severe perfusion defect	0	3	27	30
Total	169	39	30	238

Agreement 83.6%, kappa = 0.65, SE = 0.5, p < 0.001.
SPECT = single-photon emission computed tomography.

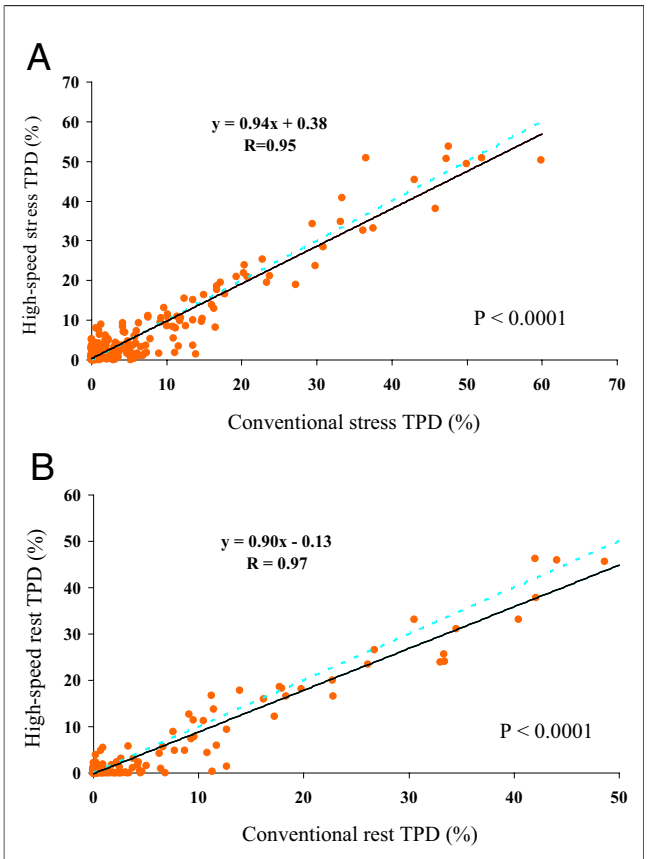

Figure 2 **Correlation of Quantitative TPD (%) by High-Speed Versus Conventional SPECT**

Stress **(A)**; rest **(B)**. **Solid lines** = regression line; **dashed lines** = identity line. TPD = total perfusion deficit; other abbreviation as in Figure 1.

methods was linear over a wide range of EF values (r = 0.89) (Fig. 6A). Bland-Altman analysis demonstrated a small average of the differences between conventional and high-speed SPECT (−0.96 ± 5.5), with no correlation between the differences and mean EF values (Fig. 6B).

Case example. Figure 7A demonstrates high-speed and conventional SPECT images of a 61-year-old man, showing a reversible defect at the anterior and apical walls, consistent with moderate ischemia in the left anterior descending coronary artery territory. Quantitative analysis yielded similar TPD values for stress and rest images of the 2 methods (Fig. 7B). Invasive coronary angiography revealed 70% stenosis at the proximal mid-left anterior descending coronary artery. High-speed SPECT images are typically characterized by better resolution with clearer edge definition, thinner ventricular walls, and larger cavity.

Discussion

This prospective, multicenter trial compared a new high-speed SPECT technology with conventional SPECT in 4 U.S. medical centers. Normal limits for quantitative analysis of MPI of the high-speed and conventional SPECT technology were developed in 63 patients with a low pre-test CAD likelihood (<15%) and used for quantitative comparison of the 2 methods in 238 patients referred for clinical evaluation of CAD. The study demonstrates comparable results for myocardial perfusion and function measurements between the 2 modalities.

Recent developments in SPECT technology. Decreasing imaging time and decreasing patient radiation exposure have become important challenges of nuclear cardiology. The principal methods used to achieve these goals have been the use of more efficient photon acquisition systems and improved reconstruction algorithms. Several approaches for new acquisition technologies have been introduced (15–22). A recent multicenter study evaluating a new solid-state cardiac camera demonstrated diagnostic performance comparable to that of standard SPECT cameras, with superior image quality and significantly shorter acquisition time (22).

In this trial, we used a novel technology, incorporating an improved photon acquisition system and a reconstruction algorithm (2–5). In a pilot clinical study (6), this system demonstrated up to 8 times increased myocardial sensitivity and higher resolution compared with a conventional SPECT system. The present study was performed in multiple centers and used quantitative analysis of SPECT MPI, providing an objective method for assessing the

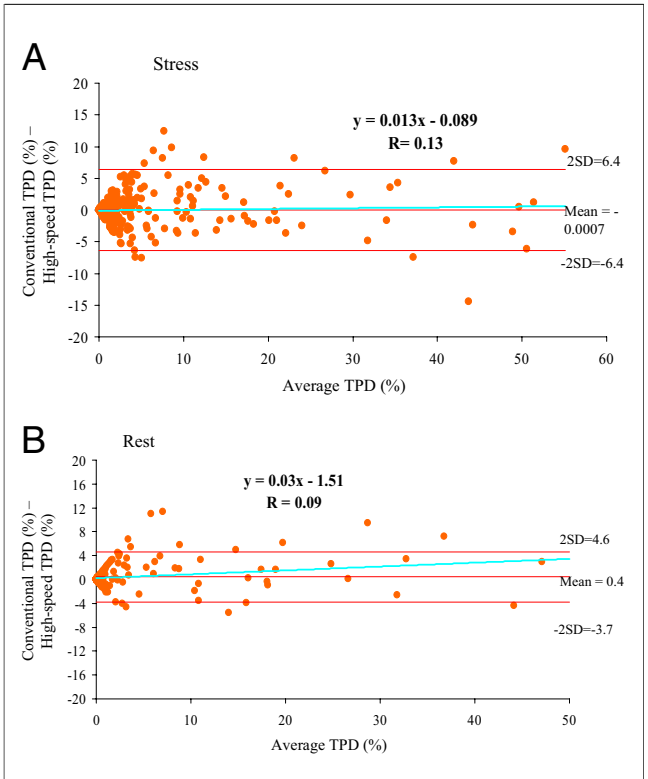

Figure 3 **Bland-Altman Plots for TPD (%) by High-Speed Versus Conventional SPECT**

Stress **(A)**; rest **(B)**. These data correspond to the data in Figure 2. Abbreviations as in Figures 1 and 2.

Table 4 TPD (%) by High-Speed Versus Conventional SPECT

	Stress				Rest			
	R	Slope	Constant	p Value	R	Slope	Constant	p Value
CSMC	0.98	0.98	0.74	<0.001	0.98	0.95	0	<0.001
BWH	0.96	0.88	0.44	<0.001	0.98	0.83	0.01	<0.001
BHM	0.91	1.02	0.60	<0.001	0.96	0.91	0.13	<0.001
VUMC	0.91	0.83	0	<0.001	0.94	0.83	−0.57	<0.001
All	0.95	0.94	0.38	<0.001	0.97	0.90	−0.13	<0.001

SPECT = single-photon emission computed tomography; TPD = total perfusion deficit; other abbreviations as in Table 1.

location and magnitude of perfusion defects. Quantitative analysis has been shown to be useful in comparing sequential MPI studies (23,24) and assessing the effectiveness of invasive as well as medical treatments in patients with CAD (25) and to provide evidence of the generalizability of the SPECT MPI results with the new system.

Normal limits. Normal variability differed between the 2 imaging technologies (Fig. 1). Some of the differences might be attributed to the sitting versus supine patient position during data acquisition, influencing the position of the attenuating tissues relative to the heart. In this regard, the high-speed system's higher count rate in the anterior and mid-inferior inferoseptal segments observed in men might be due to a lower position of the diaphragm and abdominal fat tissue, whereas the higher count rate in the anterior wall and lower count rate in the inferior segments observed in women could be explained by a lower position of the breast in the sitting position. Other differences might be due to the higher resolution of the system.

Magnitude of perfusion defects. Excellent linear correlation between quantitative TPD for high-speed and conventional SPECT in the stress and resting images demonstrated the agreement between the 2 technologies using an objective tool. Center-based analysis demonstrated good correlations at all 4 participating institutions, even though significant differences in patient clinical characteristics were observed. Differences in the male/female ratio, average age, average BMI, and pre-test CAD likelihood did not seem to affect the accuracy in

Table 5 Concordance in Coronary Artery Territories

	High-Speed SPECT		
Conventional SPECT	Normal (TPD <3%)	Abnormal (TPD ≥3%)	Total
LAD territory*			
Normal (TPD <3%)	178	10	188
Abnormal (TPD ≥3%)	11	39	50
Total	189	49	238
LCX territory†			
Normal (TPD <3%)	198	6	204
Abnormal (TPD ≥3%)	9	25	34
Total	207	31	238
RCA territory‡			
Normal (TPD <3%)	200	4	204
Abnormal (TPD ≥3%)	12	22	34
Total	212	26	238

*Agreement 91.2%, kappa = 0.73, SE = 0.055, p < 0.001. †Agreement 93.7%, kappa = 0.73, SE = 0.065, p < 0.001. ‡Agreement 93.3%, kappa = 0.70, SE = 0.071, p < 0.001.

LAD = left anterior descending coronary artery; LCX = left circumflex coronary artery; RCA = right coronary artery; SPECT = single-photon emission computed tomography.

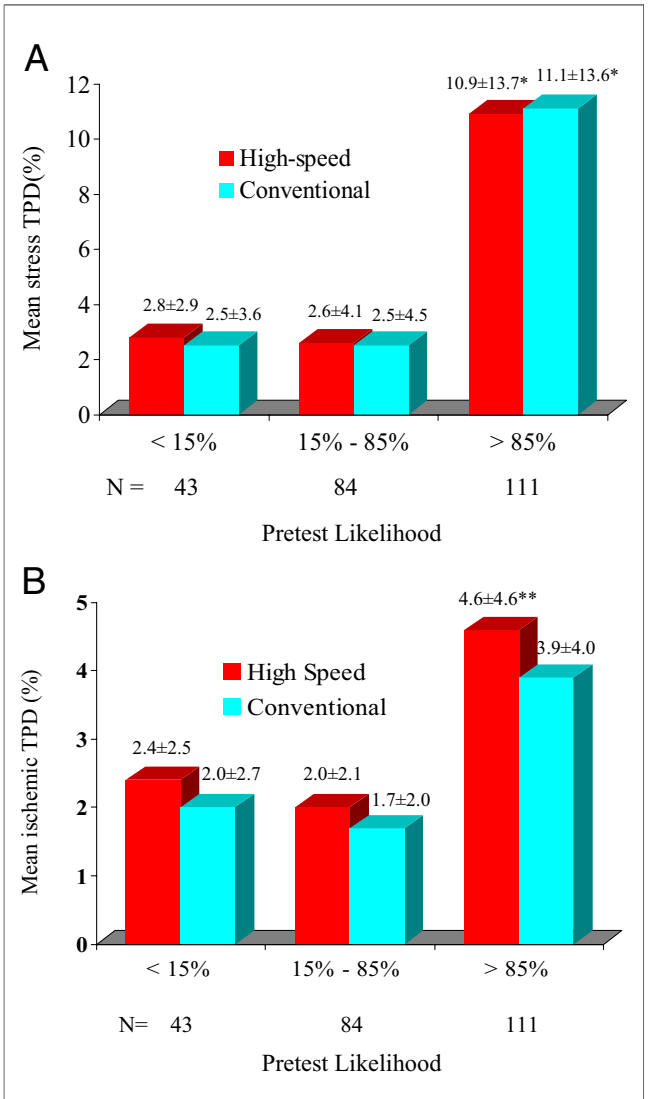

Figure 4 Perfusion Abnormality as a Function of Pre-Test Likelihood of Coronary Disease

Stress TPD (%) **(A)**; TPD ischemic (stress minus rest) **(B)** for high-speed and conventional SPECT. *p < 0.001 versus TPD of the low and intermediate pre-test likelihood category of the same imaging modality. **p < 0.05 versus conventional SPECT in the same pre-test likelihood category.

JACC Vol. 55, No. 18, 2010
May 4, 2010:1965–74

Table 6 Concordance in Reversible, Partially Reversible, and Fixed Defects

	High-Speed SPECT			
Conventional SPECT	Normal	Reversible or Mixed Defect	Fixed Defect	Total
Normal	134	11	1	146
Reversible or mixed defect	8	20	4	32
Fixed defect	2	10	5	17
Total	144	41	10	195

Agreement 81.5%.
SPECT = single-photon emission computed tomography.

detecting the amount of MPI perfusion abnormality. Furthermore, the type of gamma camera used for conventional SPECT acquisition or the radiopharmaceutical used did not affect the correlation between high-speed and conventional SPECT approaches.

The 2-SD limits for the differences in stress TPD, shown in Figure 2A, are not very narrow (±6.4%). However, comparison of different acquisitions made with 2 different camera systems would be expected to show greater variability than repeat studies performed with a 1-camera system. In addition, different attenuation patterns originating from the supine and sitting patient positions, used for the conventional and high-speed systems, respectively, might have contributed to differences in quantitative analysis of perfusion images between the 2 systems. Nevertheless, in most of the patients, the differences were small and the amount of MPI perfusion abnormality at stress and the amount of ischemia were comparable in patients with intermediate and high pre-scan likelihood of CAD. Further support of the similarity of the findings between the systems is provided by the kappa analysis, which demonstrated good concordance between the 2 imaging methods with respect to the magnitude of perfusion abnormality and localization in the 3 vascular territories.

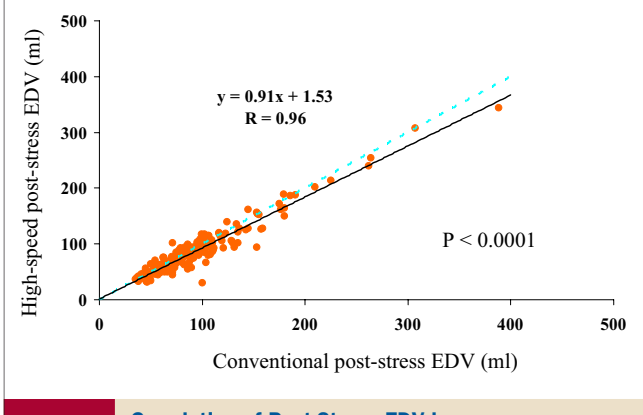

Figure 5 Correlation of Post-Stress EDV by High-Speed Versus Conventional SPECT

Solid line = regression line, **dashed line** = identity line. EDV = end-diastolic volume; SPECT = single-photon emission computed tomography.

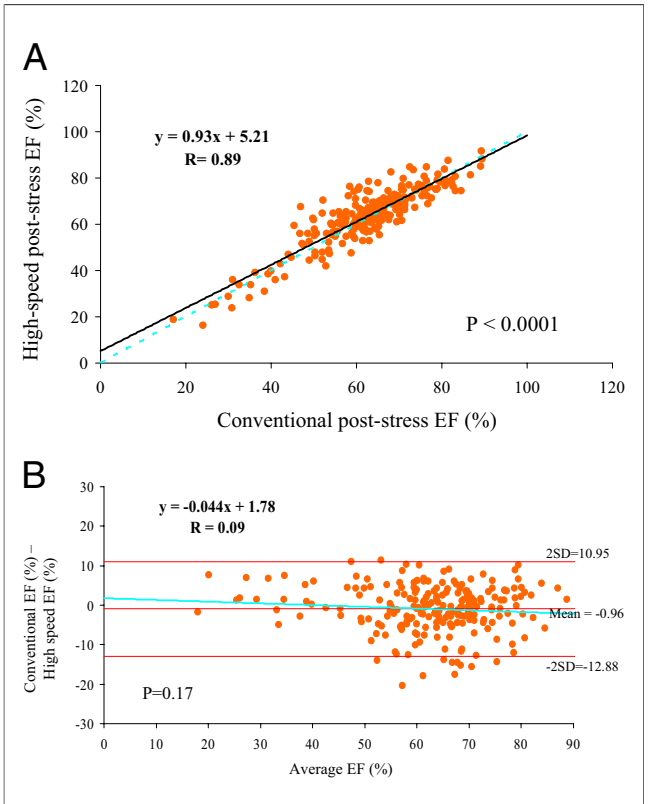

Figure 6 Post Stress EF by High-Speed Versus Conventional SPECT

(A) Correlation; **solid line** = regression line, **dashed line** = identity line. **(B)** Bland-Altman plot. EF = ejection fraction; SPECT = single-photon emission computed tomography.

Both imaging methods demonstrated a stepwise increase in TPD with increasing likelihood of CAD. A small but significantly larger amount of ischemia was seen with the high-speed system compared with conventional SPECT in patients with a high likelihood of CAD. As shown in Table 6, good agreement between the 2 imaging methods with respect to patient diagnosis having ischemia, infarct, or partially reversible defects was observed. A slight but significant underestimation of resting perfusion defects was observed with the high-speed system. The rest images were obtained after the low-dose injection and therefore have poorer count statistics than the higher dose stress images, which may have contributed to this finding.

Assessment of left ventricular function. Our study provides initial validation of gated SPECT measurements with the high-speed technology. Using QGS without constraining the valve plane motion, an action possible with the improved resolution and visibility of the basal portion of the myocardium, yielded a high correlation of post-stress EDV and EF by high-speed versus conventional SPECT over a wide range of EDV and EF values.

The limits of agreement (±2 SD) for EF were not small (11.91 EF units); however, all the outliers and most of the cases with a large difference between the 2 methods were in the

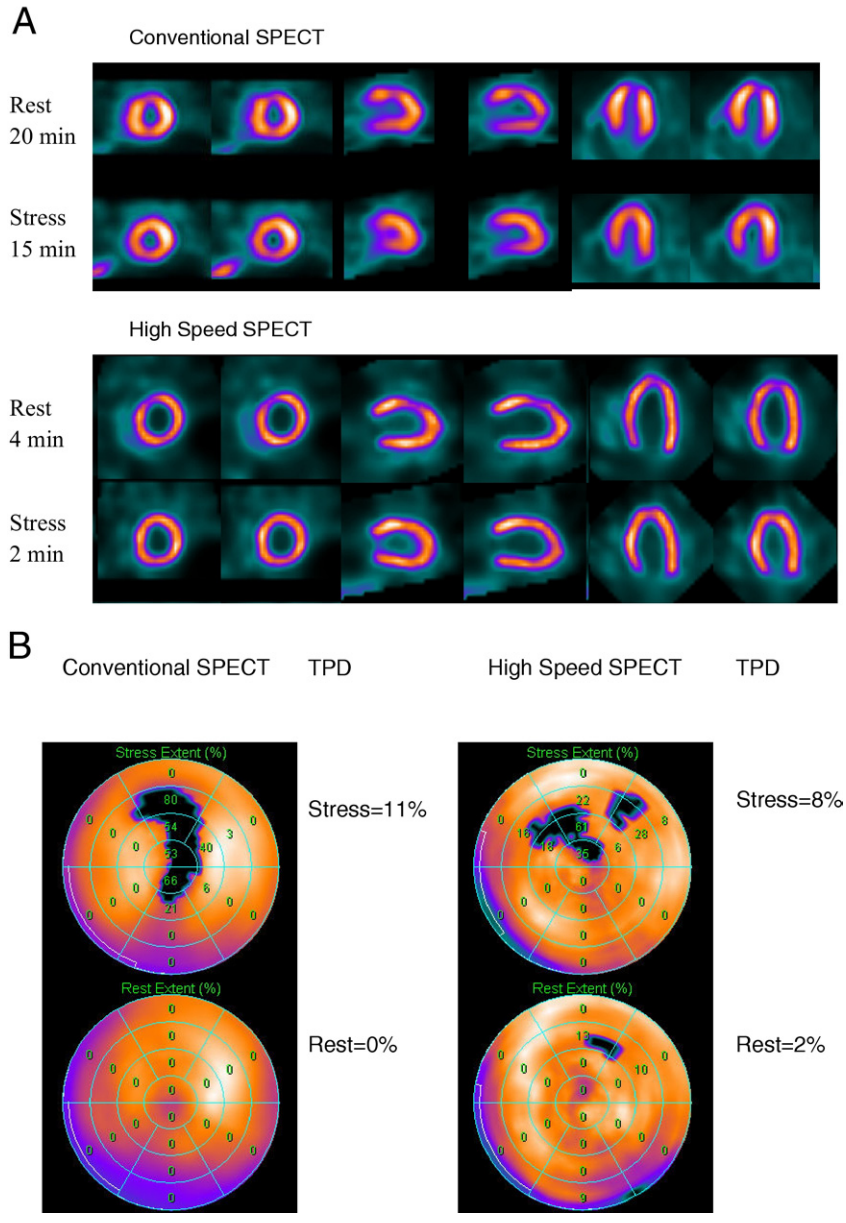

Figure 7 **Case Example of MPI of a Patient With 70% Stenosis of the Proximal Mid-Left Anterior Descending Coronary Artery**

(A) Perfusion images by conventional **(top)** and high-speed **(bottom)** SPECT demonstrating a moderate reversible perfusion defect in the left anterior descending coronary artery territory. Total acquisition time is indicated on the left-hand side. **(B)** Quantitative analysis yielded similar results for high-speed and conventional SPECT. MPI = myocardial perfusion imaging; other abbreviations as in Figures 1 and 2.

range of an EF >50% and therefore not likely to be of clinical significance. Previous studies showed similar variability in the estimation of LVEF on serial images using a single conventional camera system and demonstrated that EF measurement was affected by changes in background activity, time of imaging, and injected dose (26,27). Because the high-speed SPECT acquisitions were performed after conventional SPECT, some of these parameters might have influenced the EF estimation.

Clinical implications. The findings of this study show that SPECT MPI can be performed quickly with the high-speed SPECT system. Although it is convenient for patients to have imaging completed in 2 to 4 min, the speed of the system lends itself to protocols that would reduce both acquisition time and radiation dose. Low-dose dual-isotope procedures have recently been reported that use thallium-201 as the stress agent and Tc-99m sestamibi or tetrofosmin as the rest agent, with prolongation of acquisition times for the thallium images to 6

min while maintaining an overall rest/stress procedure time of approximately 30 min (28). Additionally, ultralow-dose Tc-99m rest/stress protocols are being explored (A. Einstein, personal communication, September 2009). Both improved reconstruction systems and new acquisition systems such as that used in this study allow an opportunity to reduce the radiation doses associated with SPECT cardiac imaging.

Study limitations. This study did not have an external validation standard such as invasive coronary angiography for comparing the accuracy of the 2 imaging modalities. Whether the new high-speed technology is superior to the conventional method for detecting the true extent of CAD was not assessed. The high rate of normal MPI might have contributed to the correlations between the methods shown in this study. Further evaluations in patient groups with larger proportions of abnormal MPI are required.

Several of the investigators have disclosed relationships with Spectrum Dynamics. However, quantitative image analysis was performed by a technologist and supervised by a nuclear cardiologist (S.H.) with no relationship to Spectrum Dynamics, and the statistical analysis was performed by the lead author (T.S.) who did not participate in the conduct of the trial.

The study was conducted using prototype high-speed equipment (beta site), resulting in a higher percentage of technical malfunctions compared with conventional SPECT systems.

Conclusions

This multicenter study demonstrated the accuracy in detecting the amount of perfusion abnormality by a new, high-speed SPECT technology. Quantitative measures of myocardial perfusion and function, obtained using normal limits specific for the new technology, correlated extremely well with respective conventional SPECT measures, acquired over as much as 8 times longer time, with no influence of patient characteristics, type of stress, or radiopharmaceutical used. These findings support the use of this technology in nuclear laboratories using various radiopharmaceutical and stress protocols, evaluating patient populations with different demographic and clinical characteristics.

Reprint requests and correspondence: Dr. Daniel S. Berman, Department of Imaging, Cedars-Sinai Medical Center, 8700 Beverly Boulevard, Room 1258, Los Angeles, California 90048. E-mail: bermand@cshs.org.

REFERENCES

1. Anger HO. Scintillation camera with multichannel collimators. J Nucl Med 1964;5:515–31.
2. Berman DS, Nagler M, Dickman D, et al. D-SPECT: A novel camera for high quantitative molecular imaging: initial description and validation. Paper presented at: The Radiological Society of North America, 91st Scientific Assembly and Annual Meeting; 2005; Chicago, IL.
3. Patton J, Sandler M, Berman D, et al. D-SPECT: a new solid state camera for high molecular imaging (abstr). J Nucl Med 2006;47:189P.
4. Spectrum Dynamics. Available at: http://www.Spectrum-Dynamics.com. Accessed February 9, 2009.
5. Gambhir SS, Berman DS, Ziffer J, et al. A novel high sensitivity rapid acquisition single photon cardiac imaging camera. J Nucl Med 2009; 50:635–43.
6. Sharir T, Ben-Haim S, Merzon K, et al. High myocardial perfusion imaging: initial clinical comparison to conventional dual detector Anger camera imaging. J Am Coll Cardiol Img 2008;1:156–63.
7. Diamond GA, Staniloff HM, Forrester JS, et al. Computer assisted diagnosis in the noninvasive evaluation of patients with suspected coronary artery disease. J Am Coll Cardiol 1983;1:444–5.
8. Shepp LA, Vardi Y. Maximum likelihood reconstruction for emission tomography. IEEE Trans Med Imaging 1982;1:113–22.
9. Lange K, Carson R. EM reconstruction algorithms for emission and transmission tomography. J Comput Assist Tomogr 1984;8:306–16.
10. Hudson HM, Larkin RS. Accelerated image reconstruction using ordered subsets of projection data. IEEE Trans Med Imaging 1994; 13:601–9.
11. Slomka PJ, Nishina H, Berman DS, et al. Automated quantification of myocardial perfusion SPECT using simplified normal limits. J Nucl Cardiol 2005;12:66–77.
12. Germano G, Kiat H, Kavanagh PB, et al. Automatic quantification of ejection fraction from gated myocardial perfusion SPECT. J Nucl Med 1995;36:2138–47.
13. Slomka PJ, Nishina H, Berman DS, et al. Automatic quantification of myocardial perfusion stress-rest change: a new measure of ischemia. J Nucl Med 2004;45:183–91.
14. Bland JM, Altman D. Statistical methods for assessing agreement between two methods of clinical measurement. Lancet 1986;1:307–10.
15. Digirad. Available at: http://www.Digirad.com. Accessed February 9, 2009.
16. Maddahi J, Mendez R, Mahmarian JJ, et al. Prospective multicenter evaluation of rapid, gated SPECT myocardial perfusion upright imaging. J Nucl Cardiol 2009;16:351–7.
17. CardiArc. Available at: http://www.CardiArc.com. Accessed February 9, 2009.
18. Funk T, Kirch DL, Koss JE, Botvinick E, Hasegawa BH. A novel approach to multipinhole SPECT for myocardial perfusion imaging. J Nucl Med 2006;47:595–602.
19. Madsen MT. Recent advances in SPECT imaging. J Nucl Med 2007;48:661–73.
20. Slomka PJ, Patton JA, Berman DS, Germano G. Advances in technical aspects of myocardial perfusion SPECT imaging. J Nucl Cardiol 2009;16:255–76.
21. Esteves FP, Raggi P, Folks RD, et al. Novel solid-state-detector dedicated cardiac camera for fast myocardial perfusion imaging: multicenter comparison with standard dual detector cameras. J Nucl Cardiol 2009;16:927–34.
22. DePuey G, Gadiraju R, Anstett F. OSEM and WBR half-time gated myocardial perfusion SPECT: a comparison to filtered backprojection. J Nucl Med 2007;48 Suppl:237P.
23. Slomka PJ, Berman DS, Germano G. Quantification of serial changes in myocardial perfusion. J Nucl Med 2004;45:1978–80.
24. Berman DS, Kang X, Gransar H, et al. Quantitative assessment of myocardial perfusion abnormality on SPECT myocardial perfusion imaging is more reproducible than expert visual analysis. J Nucl Cardiol 2009;16:45–53.
25. Shaw LJ, Berman DS, Maron DJ, et al. Optimal medical therapy with or without percutaneous coronary intervention to reduce ischemic burden: results from the Clinical Outcomes Utilizing Revascularization and Aggressive Drug Evaluation (COURAGE) trial nuclear substudy. Circulation 2008;117:1283–91.
26. Vallejo E, Chaya H, Plancarte G, Victoria D, Bialostozky D. Variability of serial same-day left ventricular ejection fraction using quantitative gated SPECT. J Nucl Cardiol 2002;9:377–84.
27. Vallejo E, Dione DP, Bruni WL, et al. Reproducibility and accuracy of gated SPECT for determination of left ventricular volumes and ejection fraction: experimental validation using MRI. J Nucl Med 2000;41:874–82.
28. Berman DS, Kang X, Tamarappoo B, et al. Stress thallium-201/rest Tc-99m sequential dual isotope high-speed myocardial perfusion imaging. J Am Coll Cardiol Img 2009;2:273–82.

Key Words: high-speed SPECT ■ myocardial perfusion imaging ■ new technology ■ quantitative analysis ■ single-photon emission computed tomography.